Role of oxygen in materials properties of yttrium trihydride

Aleksandr Pishtshev*

Institute of Physics, University of Tartu, Riia 142, 51014 Tartu, Estonia

Smagul Zh. Karazhanov

Department for Solar Energy, Institute for Energy Technology, NO-2027 Kjeller, Norway

Abstract

Numerous experiments have shown that the oxygen-free films of YH_3 possess the face-centered cubic (fcc) structure only at high pressures whereas oxygen-containing YH_3 films crystallize into the fcc lattice at ambient conditions. In this report, by means of first-principles simulations, we provide a detail understanding of the role of oxygen in stabilization of the fcc YH_3 under normal pressure. We performed the oxygen position preferences screening within the fcc unit cell along with geometrical optimization series and verified the major stability conditions. The main aggregate and electronic characteristics have been calculated in order to gain an insight into how the Y−O bond activation and coordination in the metallic matrix create new materials properties. The possibility of the compositional architecture on the base of fcc crystalline silicon and oxygen-containing YH_3 compounds has been suggested.

Keywords: A. Metal hydrides;, A. Optical materials;, D. Stability; D. Electronic properties

1. Introduction

Oxygen containing YH_3 films exhibit a unique property of a light-induced change of their optical properties[1–4], which takes place at room temperatures under normal pressure. These novel hydride materials might present interest for several practical applications such as engineering of smart windows[2] and optoelectronic devices[5]. Analysis of experimental results reveals that the oxygen impurities play an important role in structural, electronic, and optical properties of the YH_3 films. For instance, from the time-resolved X-ray diffraction studies it was found[3] that the O-containing YH_3 films possess an insulating BiF_3-type structure with face-centered-cubic (fcc) lattice (referred to as YHO hereafter). Investigations of the optical properties showed that the electronic band gap (E_g) of the YHO films varies in a wide range[1, 6].

At ambient conditions, the oxygen-free films of YH_3 crystallize in a hexagonal close-packed (hcp) structure. A fcc lattice becomes the energetically most favorable structure at the elevated pressure of about 8 GPa.[7] Studies of Machida *et al* [8, 9] demonstrated that at pressures of no less than 23 GPa, a hcp-fcc phase transition is accompanied with the electronic band gap

*Corresponding author
Email address: aleksandr.pishtshev@ut.ee (Aleksandr Pishtshev)

closure. Detailed first-principles investigations of the O-free YH_3 compounds were carried out in a number of works (see, e.g., Refs. [10, 11]). In contrast, neither the effect of chemical substitution nor structural and electronic properties have never been theoretically considered for the recently developed ternary YHO materials. Evidently, the solid understanding of the processes governing stabilization and functioning of these compounds is of crucial importance for the further progress of experimental and technological work. Thus, the main goal of the present paper is to establish the physical mechanisms underlying the oxygen-induced stabilization of the fcc structure at ambient conditions as well as to give the proper description of principal features of the electron subsystem. In particular, we will address two fundamental issues, namely, why just the oxygen atoms play the dominant role in suppression of lattice instability of the fcc phase of the O-free YH_3, and which new structural, mechanical and electronic properties are created by incorporation of a certain amount of oxygen atoms into the system of the metal host and hydrogen.

2. Structural model and computational details

Chemical background and selection of a model. Our theoretical efforts will be concentrated on the evolution of the YHO crystalline structure in terms of the oxygen content. From analysis of experimental data[3, 6, 12] one can summarize that: (i) oxygen is incorporated into yttrium hydride films during a deposition process; simultaneously, there occurs some moderate deficiency of hydrogen atoms; (ii) oxygen demonstrates high reactivity with respect to yttrium; (iii) metal-insulator transition when the unstable metallic form of fcc YH_3 transfers into the semiconducting one takes place upon oxygenation process and is irreversible; (iv) the new phase corresponds to a stable solid with a similar fcc lattice structure; and (v) to date, none of the scientific reports have given any information concerning arrangements of O-impurities in the fcc lattice of YH_3.

Taking now into account that hydration of a metal proceeds initially via hydrogen interstice positions, one can therefore suggest that uptake and fixation of oxygen in the yttrium lattice environment is the result of a competition between the diffusible oxygen and hydrogen atoms for the desired linking with yttrium atom. This effect appears in the process of interstitial dissolution and is caused by the robust chemical potential of yttrium, which, acting as a strong deoxidizer[13], tends to prevent O and H atoms from the chemical interaction with each other by binding one of them. Evidently, the irreversible incorporation of a noticeable amount of oxygen into the bulk of a Y−H system happens as a result of chemisorption and takes place inside the area enclosing a sufficient number of the dissociated oxygen and hydrogen atoms. This in turn permits a possibility of H→O substitution in the trapping process governed by the yttrium site. The ternary YHO compound formation can formally be represented in terms of the partial replacement by equation $Y + 3\,H + 2x\,O \rightarrow YH_{(3-2x)}O_x + x\,(H_2\uparrow + \frac{1}{2}\,O_2\uparrow)$, where the first term on the right side corresponds to the substitution and hydrogen off-stoichiometry effects, the second one relates to excess molecules, which are supposed to be evolved into environment. Two points should be noted in the context of the above reaction. First, the main benefit the oxygen has over the hydrogen for selectivity on binding with Y in the metallic matrix can be seen from comparison of the bond dissociation energies, namely, 7.4 eV for the Y−O bond[14] and 3.5 eV for the Y−H bond[15]. Second, as oxygen is more electronegative than hydrogen, an additional charge transfer along the new Y−O connection will give rise to a proper redistribution of the electronic density in the YHO system, which may provide an experimentally observed structural stabilization of a fcc-like phase of the oxygen doped YH_3 films.

Computational aspects. The periodic plane-wave-basis DFT simulations were carried out by using the Vienna Ab-initio Simulation Package (VASP)[16] together with the potential projector augmented-wave (PAW) method[17–19]. In the calculations the Perdew-Burke-Ernzerhof (PBE)[20] GGA exchange-correlation functional was utilized, the cutoff energy of the plane waves was set to 680 eV, and PAW pseudopotentials were adopted with $4s^2 4p^6 5s^2 4d^1$, $1s^1$, and $2s^2 2p^4$ valence electron configurations for Y, H, and O atoms, respectively. A Γ-point centered mesh for the **k**-point sampling was chosen as follows: $8 \times 8 \times 8$ for oxygen position preferences screening, geometry optimizations and stability evaluations; $16 \times 16 \times 16$ for electronic structure calculations. Theoretical modeling of an electronic structure was made at a force tolerance < 0.002 eV/Å and a convergence criterion of 1×10^{-8} eV. To narrow down the theoretical underestimation of the GGA band-gap, MetaGGA calculations with the TB-mBJ potential[21, 22] were performed with the $12 \times 12 \times 12$ **k**-point sampling. Graphic illustration of Fig. 1 was made using the VESTA program[23].

3. Results and Discussion

Structural properties of the YHO system. In order to take into account the incorporation of oxygen via the H→O substitution and, correspondingly, to model the suppression of structural instability of the undopped fcc YH_3, two hydrogen atoms occupied interstice positions of the original fcc-lattice were replaced by one oxygen atom. Such theoretical model corresponds to a chemical composition of $YH_{(3-2x)}O_x$ with $x = 0.25$, which is very close to an approximate composition of $YH_{2.4}O_{0.3}$ proposed in Ref. [3]. Next, screening of oxygen position preferences was carried out together with full geometrical optimization. The resulting choice for the oxygen position in the equilibrium lattice structure of the $YH_{2.5}O_{0.25}$ compound is presented in Fig. 1. Furthermore, note that its relaxed lattice parameter $a = 5.233$ Å agrees well with the experimental value of $a = 5.24$ Å [3].

The main structural feature of the unstable fcc form of YH_3 is that Y atoms occupy the sites of a face-centered cubic lattice, while hydrogens are distributed between two distinctive interstitial sites of the octahedral and tetrahedral types[24]. Our suggestion (examined in the present study) is that such arrangement of hydrogens is well chemically matched to allow their partial substitutions by the proper dopants that do not significantly affect the fcc lattice. As it follows from our DFT simulations, the oxygenation process tends to retain a cubic shape of the lattice structure, but fcc symmetry becomes slightly distorted due to a rather short (~ 0.016 Å) lateral drift of the face-centered yttrium atom out of the face diagonal. The off-diagonality of this distortion can be evaluated in terms of a small deviation of 1.4° from the 180° diagonal angle.

Examination of structural stability. The major results related to the stability issues of the $YH_{2.5}O_{0.25}$ structure are summarized in Table 1. It is clearly seen that in contrast to fcc type of the bulk YH_3 the same compound doped heavily by oxygen, $YH_{2.5}O_{0.25}$, is dynamically and mechanically (intrinsically) stable. In particular, the lowest value of optical frequencies evaluated in a Γ-point, 154 cm^{-1}, is positive. The values of three independent elastic constants C_{11}, C_{12}, and C_{44} obey all necessary stability criteria for cubic crystals[25]: all of them are positive, and the inequality $C_{11} > C_{12}$ is satisfied. Note that the calculated values of quantities, which represent the elastic behavior, strength and stiffness characteristics, fall within the typical range related to ion-covalent insulating oxides. The bulk $YH_{2.5}O_{0.25}$ is quite well compressible ($\nu = 0.20$) and more resistant to a volume change over a shape change ($B/G > 1$). A Zener ratio of 1.64 (Table 1), which

Table 1: Frequency of low-lying zone center optical vibration Ω_0 (in cm^{-1}), and three linearly independent components of the elasticity tensor C_{ij} (in GPa) calculated for the $YH_{2.5}O_{0.25}$ structure. The macroscopic effective elastic parameters represented by the bulk (B), shear (G) and Young's (E) moduli (in GPa), and Poisson's ratio (ν) were estimated in terms of the Voigt-Reuss-Hill scheme[26]. In the last columns the dimensionless Zener ratio[27] $Z = 2C_{44}/(C_{11} - C_{12})$ is indicated. For comparison, the elastic characteristics of cubic phase of single-crystal yttria Y_2O_3 and diamond cubic Si are quoted in the second and third rows, respectively. Mismatch degrees between the elastic characteristics of $YH_{2.5}O_{0.25}$ and fcc Si are shown in the last raw.

	Ω_0	C_{11}	C_{12}	C_{44}	B	G	E	ν	Z
$YH_{2.5}O_{0.25}$	154	166.7	62.2	85.8	97.0	70.3	169.9	0.21	1.64
Y_2O_3:									
Ref. [28]					135.7	66.5	171.5	0.30	
Ref. [29]		223.7	112.4	74.6	149.5(±1.0)	66.3(±0.8)	173.0(±2.0)	0.31	1.34
Ref. [30]					148.9(±3.0)	69.2(±2.0)	179.8(±4.8)	0.30	
fcc Si:									
Ref. [31]		165.6	63.9	79.5	97.8	66.5	162.5	0.22	1.56
Mismatch with respect to fcc Si		0.66%	2.66%	7.92%	0.82%	5.71%	4.55%		

provides an important measure of an elastic anisotropy in materials of a cubic structure, noticeably deviates from 1, i.e. from the condition of the isotropic elasticity. Correspondingly, one can surely predict for YHO systems the existence of oxygen content dependent anisotropy in the thermal expansion effect. Interesting point is that the shear and Young's moduli of $YH_{2.5}O_{0.25}$ and Y_2O_3 are very similar – both materials demonstrate nearly identical rigidity and stiffness. Undoubtedly, such alignment of aggregate characteristics confirms the key role the strength and rigidness of additional Y−O bonds play in establishing crystalline stability of $YH_{2.5}O_{0.25}$.

Next step was an analysis of an oxygen role in the bulk YHO system with $2 \times 2 \times 1$ supercell computer simulations, which has indicated that dynamic stabilization of the fcc lattice can be already achieved at oxygen doping level as low as $x = 0.0625$.

Another promising feature of the compound studied is that its aggregate properties (Table 1) are similar to those reported in Ref. [31] for fcc silicon, a typical material of semiconductor devices. Moreover, as follows from our computer simulations the lattice parameter of the YHO system is modulated via the oxygen content, so that, taking into account that the lattice constant of silicon is 5.431 Å [31], it could be possible to reduce the small mismatch (3.65%) of the lattice parameters between both materials. In the context of the fabrication process, it may be assumed that these two factors could give possibilities for getting novel hybrid designs, such as, for instance, the high-quality depositions on a fcc-type single-crystalline silicon substrate.

Electronic properties. Electronic structure calculations carried out for two different oxygen concentrations have demonstrated that the induced lattice stabilization is accompanied by the transition of the system from the metallic unstable to the semiconducting stable state (Table 2). Regardless of the fact that GGA-DFT approach gives a lower-bound estimate for the gap in the electron spectrum, comparison of the data of Table 2 reveals the direct dependence of the E_g value on the amount of incorporated oxygen. This in turn gives a theoretical confirmation of experimentally found possibility[6] to manipulate the magnitude of the forbidden gap in the YHO system by dealing with arrays of oxygen atoms and hydrogen off-stoichiometry during the fabrication process. MetaGGA calculations with the TB-mBJ potential have given for the

Table 2: Theoretical predictions of fundamental band gaps (in eV) for two different contents of oxygen.

Compound	PBE	TB-mBJ
$YH_{2.5}O_{0.25}$	2.0	3.2
$YH_{2.875}O_{0.0625}$	0.6	–

fundamental band gap of the $YH_{2.5}O_{0.25}$ compound the value of 3.2 eV, which lies in the range $2.6 < E_g < 4$ eV observed in samples with different levels of oxygenation[4].

Figure 2 shows that the $YH_{2.5}O_{0.25}$ material has a direct band gap with the valence band (VB) maximum and the conduction band (CB) minimum located at the L-point of the Brillouin zone. The band gap at the Γ-point is larger by ∼0.6 eV. The total density of states is shown in Figure 3 together with orbital-site projected density of states (PDOS). The central feature of the electronic spectra of $YH_{2.5}O_{0.25}$ is two regions located in the upper part of the VB at 0 to −2 eV and −2 to −4 eV. Both are composed of occupied sp^3d-type strongly hybridized states of hydrogen, oxygen and yttrium, respectively, but differ markedly by peak shapes. Regarding the genesis of optical spectrum and frequency profile of the optical parameters of $YH_{2.5}O_{0.25}$ one can therefore predict that, along with high-intensive $4d$ empty states of yttrium, which contribute predominately to the lowest part of the CB, sp^3-character of the highest occupied band will be mainly responsible for governing dipolar selection rules for electronic transitions starting from the fundamental absorption edge. Moreover, as also seen from yttrium PDOS of Figure 3, for higher exciting energies, the dipole transition matrix elements will start in addition to select Y s-related states in the CB.

4. Conclusion

In this work, we have demonstrated that the higher chemical susceptibility of an yttrium atom to oxygen than to hydrogen plays a key role in the effect of oxygen-caused stabilization of fcc YH_3 crystalline films. If some oxygen amount is incorporated into the metal matrix during the metal hydride formation process, the Y atoms tend to prevent the water reaction by trapping the oxygens into interstice hydrogen positions. By using DFT computer simulations, we have shown that such establishment of the stable Y−O connections correctly interprets the experimental results. We have also investigated in terms of DOS and band picture how the oxygenation potential is manifested in the electronic properties of the bulk YHO material. The following distinctive features related to the electron structure of the YHO material are resulted from our calculations: (i) it is direct band gap semiconductors, and (ii) the band gap value is straightforwardly dependent on the incorporated oxygen amount that was irreversible trapped by yttrium atoms. The last feature greatly facilitates possibilities to band gap engineering by varying oxygen and hydrogen contents. On the base of comparison of the calculated elastic and structural characteristics with those of fcc silicon, it was suggested that the YHO material with the oxygen content close to the value of 0.25 could be well integrated with silicon to design an architecture of novel hybrid solid-state electronic devices.

In summary, by gathering together the experimental and theoretical data, one can conclude that the YHO system is technologically flexible material whose practical usefulness lies in possibilities to manipulate its structural and electronic properties via the oxygenation and hydrogen off-stoichiometry effects.

5. Acknowledgements

This work has received financial and supercomputing support from the Research Council of Norway within the FME project (192839) and ISP NANOMAT project (181884) as well as it was supported by the European Union through the European Regional Development Fund (Centre of Excellence "Mesosystems: Theory and Applications", TK114) and by the Estonian Science Foundation (grant No 7296).

References

References

[1] T. Mongstad, C. Platzer-Björkman, J. P. Maehlen, L. P. Mooij, Y. Pivak, B. Dam, E. S. Marstein, B. C. Hauback, S. Z. Karazhanov, A new thin film photochromic material: Oxygen-containing yttrium hydride, Solar Energy Mater. Solar Cells 95 (2011) 3596–3599.

[2] T. Mongstad, "Thin-film metal hydrides for solar energy applications", Phd thesis, The University of Oslo, Oslo, Norway (2012).

[3] J. P. Maehlen, T. T. Mongstad, C. C. You, S. Karazhanov, Lattice contraction in photochromic yttrium hydride, J. Alloys Compd. 580 (2013) S119–S121.

[4] T. Mongstad, A. Thøgersen, A. Subrahmanyam, S. Karazhanov, Characterisation of the photochromic effect in metal hydride thin films, Solar Energy Mater. Solar Cells (2014) Accepted for publication.

[5] M. Pärs, K. Gräf, P. Bauer, M. Thelakkat, J. Köhler, Optical gating of perylene bisimide fluorescence using dithienylcyclopentene photochromic switches, Appl. Phys. Lett. 103 (2013) 221115.

[6] C. C. You, T. Mongstad, J. P. Maehlen, S. Karazhanov, Engineering of the band-gap and optical properties of thin films of yttrium hydride, Appl. Phys. Lett. (2014) submitted.

[7] T. Palasyuk, M. Tkacz, Hexagonal to cubic phase transition in YH_3 under high pressure, Solid State Commun. 133 (2005) 477–480.

[8] A. Machida, A. Ohmura, T. Watanuki, T. Ikeda, K. Aoki, S. Nakano, K. Takemura, X-ray diffraction investigation of the hexagonal-fcc structural transition in yttrium trihydride under hydrostatic pressure, Solid State Commun. 138 (2006) 436–440.

[9] A. Ohmura, A. Machida, T. Watanuki, K. Aoki, S. Nakano, K. Takemura, Infrared spectroscopic study of the band-gap closure in YH_3 at high pressure, Phys. Rev. B 73 (2006) 104105.

[10] D. Y. Kim, R. H. Scheicher, R. Ahuja, Predicted High-Temperature Superconducting State in the Hydrogen-Dense Transition-Metal Hydride YH_3 at 40 K and 17.7 GPa, Phys. Rev. Lett. 103 (2009) 077002.

[11] R. Ahuja, B. Johansson, J. Wills, O. Eriksson, On the semiconducting state and structural properties of YH_3 from first principles theory, Appl. Phys. Lett. 71 (1997) 3498–3500.

[12] T. Mongstad, C. Platzer-Björkman, J. P. Maehlen, B. C. Hauback, S. Z. Karazhanov, F. Cousin, Surface oxide on thin films of yttrium hydride studied by neutron reflectometry, Appl. Phys. Lett. 100 (2012) 191604.

[13] C. A. Lensing, Y. D. Park, I. S. Maroef, D. L. Olson, Yttrium hydrogen trapping to manage hydrogen in HSLA steel welds, Welding Journal 83 (2004) 254–S–266–S.

[14] Properties of atoms, radicals, and bonds, in: J. Dean (Ed.), Lange's Handbook of Chemistry, 15th edn, McGraw-Hill, 1999, book section Section 4, p. 4.1.

[15] K. Balasubramanian, J. Z. Wang, Spectroscopic properties and potential energy curves of 29 electronic states of YH, Journal of Molecular Spectroscopy 133 (1989) 82–89.

[16] G. Kresse, J. Furthmüller, Efficient iterative schemes for ab initio total-energy calculations using a plane-wave basis set, Phys. Rev. B 54 (1996) 11169–11186.

[17] P. E. Blöchl, Projector augmented-wave method, Phys. Rev. B 50 (1994) 17953–17979.

[18] G. Kresse, D. Joubert, From ultrasoft pseudopotentials to the projector augmented-wave method, Phys. Rev. B 59 (1999) 1758–1775.

[19] G. Kresse, J. Hafner, Ab initio molecular dynamics for liquid metals, Phys. Rev. B 47 (1993) 558–561.

[20] J. P. Perdew, K. Burke, M. Ernzerhof, Generalized gradient approximation made simple, Phys. Rev. Lett. 77 (1996) 3865–3868.

[21] F. Tran, P. Blaha, Accurate band gaps of semiconductors and insulators with a semilocal exchange-correlation potential, Phys. Rev. Lett. 102 (2009) 226401.

[22] D. Koller, F. Tran, P. Blaha, Merits and limits of the modified Becke-Johnson exchange potential, Phys. Rev. B 83 (2011) 195134.

[23] K. Momma, F. Izumi, *VESTA3* for three-dimensional visualization of crystal, volumetric and morphology data, J. Appl. Crystallogr. 44 (2011) 1272–1276.
[24] J. P. Dekker, J. van Ek, A. Lodder, J. N. Huiberts, The gap in YH_3 and its lattice structure, J. Phys.: Condens. Matter 5 (1993) 4805.
[25] R. A. Cowley, Acoustic phonon instabilities and structural phase transitions, Phys. Rev. B 13 (1976) 4877–4885.
[26] R. Hill, The elastic behaviour of a crystalline aggregate, Proc. Phys. Soc. Sect A 65 (1952) 349.
[27] J. Lalena, D. Cleary, M. Weiser, Principles of Inorganic Materials Design, Wiley, 2010.
[28] R. Munro, Elastic moduli data for polycrystalline ceramics, in: NISTIR, National Institute of Standards and Technology, Gaithersburg, 2002, p. 6853.
[29] J. W. Palko, W. M. Kriven, S. V. Sinogeikin, J. D. Bass, A. Sayir, Elastic constants of yttria Y_2O_3 monocrystals to high temperatures, J. Appl. Phys. 89 (2001) 7791–7796.
[30] O. Yeheskel, O. Tevet, Elastic moduli of transparent yttria, Journal of the American Ceramic Society 82 (1999) 136–144.
[31] A. George, Elastic constants and moduli of diamond cubic Si, in: R. Hull (Ed.), Properties of Crystalline Silicon, INSPEC, London, 1997, p. 98.

FIGURES

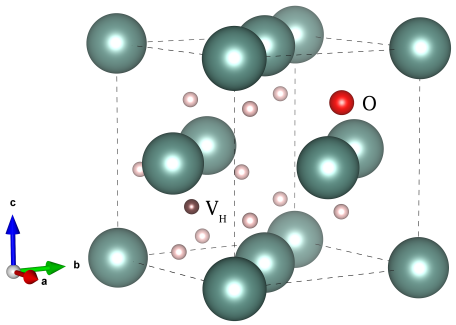

Figure 1: Schematic presentation of the fcc $YH_{2.5}O_{0.25}$ structure. The relaxed lattice constant a = 5.233 Å. Y atoms are sketched by the large green color balls. The preferred oxygen position denoted by the red color ball corresponds to a slightly distorted tetrahedral site $(0.7470, 0.7470, 0.7470)$ that is very close to the nominal site at $(\frac{3}{4}, \frac{3}{4}, \frac{3}{4})$. The brown color ball depicts schematically the hydrogen V_H that was eliminated from the second tetrahedral position at $(\frac{1}{4}, \frac{1}{4}, \frac{1}{4})$.

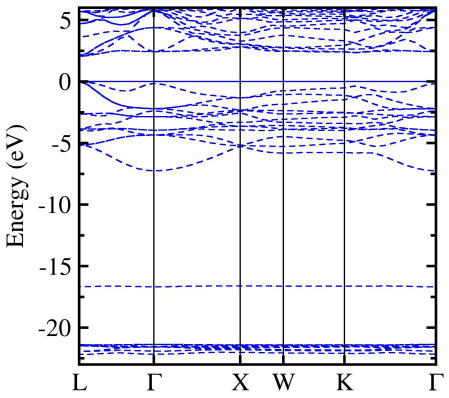

Figure 2: Electronic band structure of $YH_{2.5}O_{0.25}$ calculated with PBE-GGA functional. The Fermi level is set to zero.

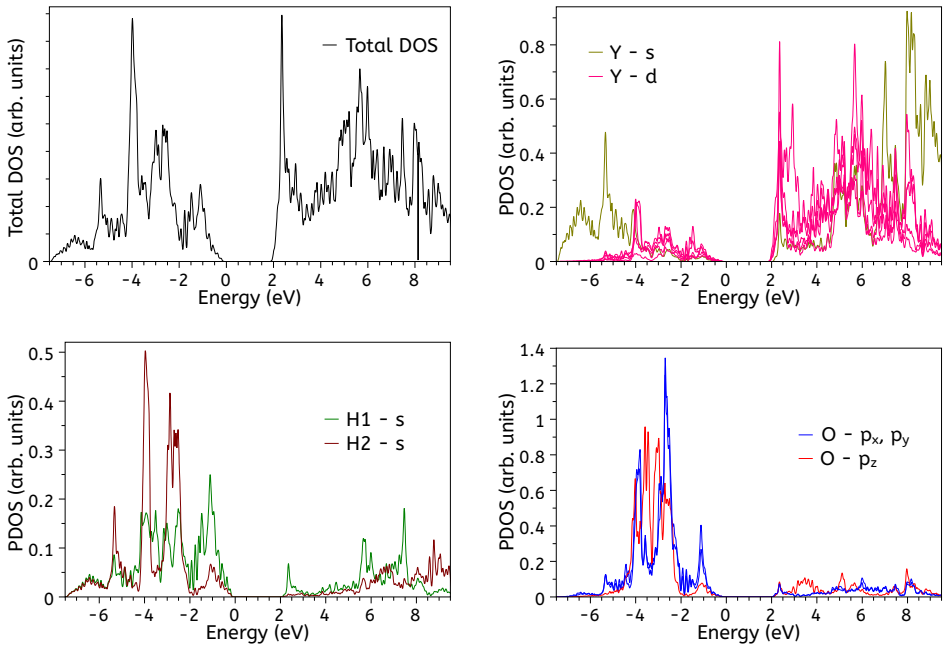

Figure 3: Total and partial density of states for $YH_{2.5}O_{0.25}$ calculated with PBE-GGA functional. The Fermi level is set to zero. PDOS depicts only those of electronic states of elements that are actual for further analysis. H1 and H2 denote *s* electronic orbitals related to hydrogen occupied the octahedral and tetrahedral sites, respectively.

Captions

Fig. 1 Schematic presentation of the fcc $YH_{2.5}O_{0.25}$ structure. The relaxed lattice constant $a = 5.233$ Å. Y atoms are sketched by the large green color balls. The preferred oxygen position denoted by the red color ball corresponds to a slightly distorted tetrahedral site $(0.7470, 0.7470, 0.7470)$ that is very close to the nominal site at $(\frac{3}{4}, \frac{3}{4}, \frac{3}{4})$. The brown color ball depicts schematically the hydrogen V_H that was eliminated from the second tetrahedral position at $(\frac{1}{4}, \frac{1}{4}, \frac{1}{4})$.

Fig. 2 Electronic band structure of $YH_{2.5}O_{0.25}$ calculated with PBE-GGA functional. The Fermi level is set to zero.

Fig. 3 Total and partial density of states for $YH_{2.5}O_{0.25}$ calculated with PBE-GGA functional. The Fermi level is set to zero. PDOS depicts only those of electronic states of elements that are actual for further analysis. H1 and H2 denote s electronic orbitals related to hydrogen occupied the octahedral and tetrahedral sites, respectively.

Table 1 Frequency of low-lying zone center optical vibration Ω_0 (in cm^{-1}), and three linearly independent components of the elasticity tensor C_{ij} (in GPa) calculated for the $YH_{2.5}O_{0.25}$ structure. The macroscopic effective elastic parameters represented by the bulk (B), shear (G) and Young's (E) moduli (in GPa), and Poisson's ratio (ν) were estimated in terms of the Voigt-Reuss-Hill scheme[26]. In the last columns the dimensionless Zener ratio[27] $Z = 2C_{44}/(C_{11} - C_{12})$ is indicated. For comparison, the elastic characteristics of cubic phase of single-crystal yttria Y_2O_3 and diamond cubic Si are quoted in the second and third rows, respectively. Mismatch degrees between the elastic characteristics of $YH_{2.5}O_{0.25}$ and fcc Si are shown in the last raw.

Table 2 Theoretical predictions of fundamental band gaps (in eV) for two different contents of oxygen.

***Highlights (for review)**

- The mechanism of oxygen-caused stabilization of fcc YH_3 compound is presented.
- The structural and electronic properties are reported.
- The possibility for band gap engineering by varying oxygen content is proposed.